

Importance of Lunar Granite and KREEP in Very High Potassium (VHK) Basalt Petrogenesis

Clive R. Neal and Lawrence A. Taylor

Department of Geological Sciences, University of Tennessee, Knoxville, TN 37996

Marilyn M. Lindstrom*

Department of Earth and Planetary Sciences, Washington University, St. Louis, MO 63130

**Now at NASA Johnson Space Center, Code SN2, Houston, TX 77058*

Five new Very High Potassium (VHK) basalts, from Apollo 14 breccia 14303, extend the compositional ranges of previously reported VHK basalts. It is demonstrated that although lunar granite is essential in achieving VHK compositions, a KREEP component is also present in the 14303 VHK basalts. An Assimilation and Fractional Crystallization model (AFC) is presented whereby a primitive magma [represented by a high-Al (HA) mare basalt composition] undergoing AFC with KREEP comes into contact with granite during migration. It is envisaged that VHK parental magmas lie along the mare basalt evolution path (Neal *et al.*, 1987a). The VHK compositions diverge from this trend because of the effect of granite assimilation. This process stresses the significance of granite in the lunar crust. Proportions of fractionating phases vary according to the position along the mare basalt evolutionary path prior to granite assimilation and can be constrained by major element modeling. The presence of VHK basalts containing only a granite signature (i.e., representing two-component AFC) and those with both granite and KREEP signatures (three-component AFC) argues for at least two different VHK basalt flows at the Apollo 14 site. An impact melt of similar composition to the VHK basalts (14303,277) is also reported and can only be distinguished on the basis of whole-rock chemistry.

INTRODUCTION

The study of mare basalts is critical in determining the nature of the lunar interior. Calculations of source compositions for these basalts and comparisons with other lunar rock types allow the extent of igneous processes, such as partial melting, fractional crystallization, and assimilation, to be evaluated with regard to the evolution of the Moon (Nyquist *et al.*, 1979; Ringwood and Kesson, 1976; Sbervais *et al.*, 1985a). For example, assimilation of a KREEP component has been invoked to explain certain anorthosite compositions (Warren *et al.*, 1983a) as well as mare basalt evolution (Binder, 1982, 1985; Dickinson *et al.*, 1985; Sbervais *et al.*, 1985a; Neal *et al.*, 1987a).

The recognition of Very High Potassium (VHK) mare basalts in Apollo 14 breccias (Sbervais *et al.*, 1985b) created problems in achieving such compositions by partial melting and/or fractional crystallization (Shih *et al.*, 1986, 1987). VHK basalts would seem to require a unique source region that, as implied by the rarity of VHK basalts, was highly localized. Major element compositions are remarkably similar to High Aluminum (HA) mare basalts except for the characteristically elevated K₂O contents (>0.5 wt %). Consequently, VHK basalts are also characterized by K₂O/Na₂O ratios of >1 and K/La ratios between 500 and 1500 (Sbervais *et al.*, 1985b). In addition, Rb and Ba are enriched relative to other HA mare basalts. In an isotopic study of two VHK basalt clasts, Shih *et al.* (1986) reported the most radiogenic ⁸⁷Sr/⁸⁶Sr values to date from the Moon, but with initial ratios indistinguishable from other analyzed basalts. More recent studies by Shih *et al.* (1987) of 14304 VHK basalts reported similar conclusions. This indicates an approximate 15-fold enrichment of Rb in the VHK magma relative to HA mare basalts at the time of crystallization.

The above observations have led to the formulation of two hypotheses to explain the production of VHK basalts: (1) a metasomatized source for the VHK basalts that is similar to that of other HA basalts but is enriched in K, Rb, and Ba (e.g., Goodrich *et al.*, 1986); and (2) assimilation of lunar granite by an HA basaltic magma (e.g., Sbervais *et al.*, 1985b). However, both hypotheses have serious shortcomings. For instance, it is unlikely that a metasomatizing fluid enriched in volatiles would also be enriched in Ba; enrichment in other volatiles besides K and Rb would also be expected (see Sbervais *et al.*, 1985b). The high U and Th contents of most lunar granites pose a mass balance problem for any simple granite assimilation model (Sbervais *et al.*, 1985b; Warren *et al.*, 1986), reflected in the normally low U and Th contents of VHK basalts. This has led to the explanation by Shih *et al.* (1987) that granitic feldspars are preferentially assimilated during VHK basalt petrogenesis. There exists yet a third possibility to explain the VHK petrogenesis wherein these basalts are the products of meteorite impact melts (G. Ryder and R. Schmitt, personal communication, 1987). This hypothesis is based upon Ni/Co ratios, Au and Ir abundances, and geochemical comparisons with the breccia matrix. These considerations will be discussed in detail within the chemistry and modeling sections below.

In this paper, we report the results of a study of five new VHK basalts from Apollo 14 breccia 14303 that form part of an ongoing investigation into VHK basalt petrogenesis (e.g., Neal *et al.*, 1987b). A sixth clast is very similar, but evidence presented below suggests it is an impact melt. The new data are compared and contrasted with previously reported VHK compositions, and the role of KREEP and lunar granite in generating all reported VHK compositions is evaluated. The ultimate aim of this research is to clarify the processes involved in VHK petrogenesis.

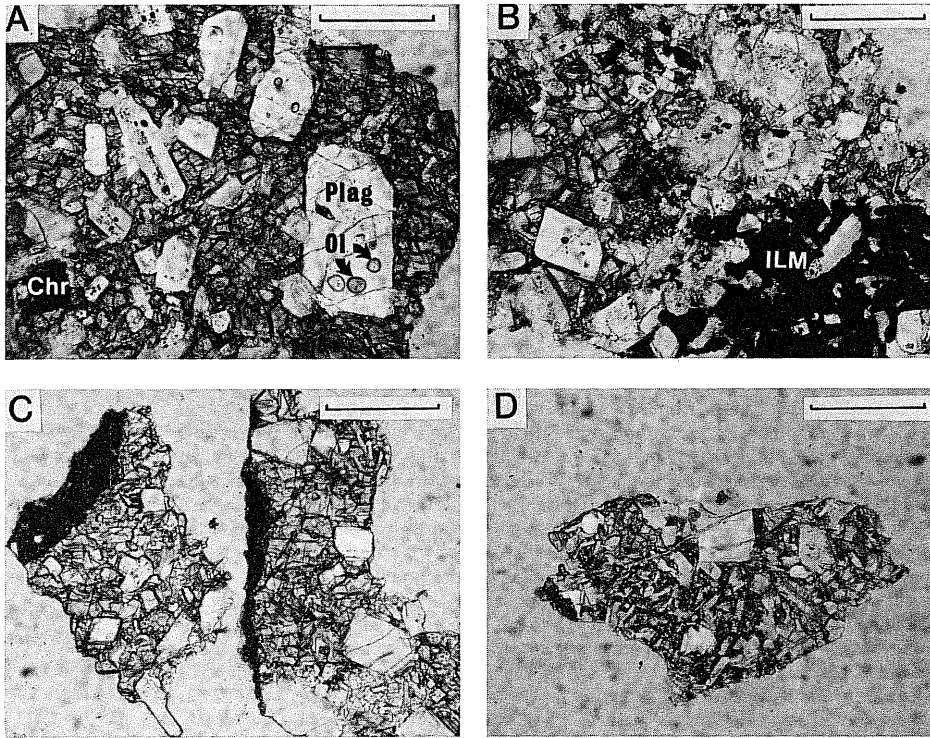


Fig. 1. Photomicrographs of the 14303 VHK basalts. The scale bar represents 0.5 mm. (a) 14303,245 contains plagioclase phenocrysts with rounded olivine inclusions, suggesting a precursory cotectic magma. One grain of chromite is seen. (b) Interstitial ilmenite in 14303,245 containing plagioclase phenocrysts. (c) Texture of 14303,246 with plagioclase phenocrysts and interstitial pyroxene. (d) Texture of 14303,249 also exhibiting plagioclase phenocrysts and interstitial pyroxene.

PETROGRAPHY AND MINERAL CHEMISTRY

Six VHK basalt clasts were extracted from Apollo 14 breccia 14303. They were small (0.25-1 cm diameter) with grain sizes reaching a maximum of 0.4 mm. Probe mounts (PM) were made for ,245 (INAA = ,244) ,246 (INAA = ,247) and ,249; in addition, probe mounts were made from "hot" INAA samples for ,266 ,275 and ,277. Mineral chemistry was determined using an automated MAC 400S electron microprobe at the University of Tennessee. Standards, operating procedures, and techniques of data reduction have been reported elsewhere (e.g., *Sbervais et al.*, 1984).

The VHK clasts from breccias 14303 are fine- to medium-grained basalts with a general subophitic texture (Fig. 1). Estimated modal abundances were determined by careful examination of each probe mount (Table 1); small sample size renders detailed point counting less than realistic. The mineralogy in ,245 is especially dominated by feldspar ($\cong 60\%$) with relatively little pyroxene ($\cong 22\%$) and olivine ($\cong 10\%$).

TABLE 1. Estimated modal proportions for the 14303 VHK basalts.

.PM No.	Feldspar	Olivine	Pyroxene	Oxide	Glass
,245	60	3	21	10	6
,246	50	0	42	3	5
,249	60	0	30	4	6
,266	40	10	30	12	8
,275	50	0	43	4	3
,277	35	15	30	15	5

Plagioclase is also the dominant phase in all other samples (except ,277), although the proportion of mafic minerals increases. The proportions of interstitial glass shows little variation throughout the suite ($\cong 3-8\%$).

Large plagioclase phenocrysts ($\cong 0.4$ mm diameter) occur in four of our samples (,245 ,246 ,249 ,275) with core compositions of An96-97 (Table 2), but they become more sodic toward the rims (An84-87). There is also a smaller, compositionally indistinguishable, groundmass plagioclase generation displaying similar zonation. The remaining two samples (,266 and ,277) have no plagioclase phenocrysts. K-feldspar is present in all samples (Table 3), except ,245, as small crystals (<0.1 mm) in interstitial K-rich glass and also as thin overgrowths on plagioclase (Or 77-93 in ,246; 82-94 in ,249; 88-92 in ,266; 86-96 in ,275; 85-95 in ,277). These K-feldspars are generally rich in Ba (0.12-5.11 wt % BaO). The petrographic relations indicate K-feldspar is a late-stage crystallization product in these basalts. Interstitial K-rich glass containing Ba is present in all six 14303 VHK basalts (Table 4). The composition of this interstitial glass in ,245 is distinct from other samples in that it has elevated FeO contents (7.09 wt %). This glass composition may be due to the lack of substantial crystallization of late-stage fayalitic olivines, possibly implying faster cooling rates for this sample. The larger grain size of the plagioclase phenocrysts in ,245, coupled with the lack of K-feldspar, again suggests that this sample has undergone greater pre-eruption fractionation and cooled more quickly after eruption, thus inhibiting K-feldspar and fayalite crystallization from interstitial liquid.

TABLE 2. Representative plagioclase analyses from 14303 VHK basalts.

PM No	,245	,246	,249	,266	,275	,277
INAA NO.	,244	,247	-	,266	,275	,277
SiO ₂	45.4	45.0	44.8	45.2	46.5	45.6
Al ₂ O ₃	34.8	35.3	35.5	34.8	34.6	34.2
FeO	0.32	0.06	0.14	0.70	0.04	0.79
CaO	18.7	18.5	18.9	17.7	17.8	18.2
Na ₂ O	0.93	0.96	0.82	0.99	1.29	1.03
K ₂ O	0.14	0.11	0.10	0.14	0.11	0.15
Total	100.29	99.93	100.26	99.53	100.34	99.97
<i>Formula moles based on eight oxygens</i>						
Si	2.091	2.075	2.065	2.097	2.129	2.109
Al	1.887	1.919	1.928	1.898	1.869	1.863
Fe	0.012	0.001	0.005	0.027	0.001	0.030
Ca	0.923	0.917	0.931	0.880	0.871	0.902
Na	0.082	0.085	0.071	0.088	0.114	0.092
K	0.006	0.005	0.005	0.006	0.005	0.008
Total	5.000	5.002	5.006	4.997	4.991	5.004
An	91.3	91.1	92.4	90.3	88.0	90.0
Ab	8.1	8.4	7.1	9.1	11.5	9.2
Or	0.6	0.5	0.5	0.6	0.5	0.8

Olivine is present only in ,245, ,266 and ,277 with two generations present, Mg- and Fe-rich, as noted by *Sbervais et al.* (1985b) from 14305 VHK basalts. In ,245 olivine occurs as two corroded (≈ 0.1 mm) grains (Fo51-52 and Fo70) (Table 5). Olivine is more common in 266 (Fo34-39 and Fo65-69) and 277 (Fo37-43 and Fo55-65), occurring as corroded phenocrysts (≈ 0.25 mm). However, also in sample ,245, some of the larger plagioclase phenocrysts contain inclusions of

olivine (Figs. 1a,b and Table 5) that are quite variable in Fo content (55-73) and span the compositional gap reported by *Sbervais et al.* (1985b). The rimming of olivine by pigeonite in all three samples, where olivine is not present as inclusions in plagioclase, indicates a reaction between olivine and melt. No pigeonite rims are present on the olivine inclusions in plagioclase of ,245.

Pyroxene compositions range from orthopyroxene to augite (Table 6 and Fig. 2), and although there is some evidence of augite rimming pigeonite, the small grain size of these samples makes the exact relationship between these phases unclear. Generally there are two pyroxene populations: Ca- and Mg-rich. The ranges in composition are displayed in Figs. 2a-f and 3a-f. In Figs. 3d and 3f (samples ,266 and ,277), the Al/Ti ratio of the pyroxenes decreases with Mg#, generally between Mg and Ca pyroxenes. This suggests plagioclase crystallization after subcalcic augite (*Bence and Papike, 1972*), similar to pyroxenes from 14305 VHK basalts. In Fig. 3e (14303,245), the Al/Ti ratio remains constant at approximately

TABLE 3. Representative orthoclase analyses from the 14303 VHK basalts.

PM No.	,246	,249	,266	,275	,277
INAA No.	,247	-	,266	,275	,277
SiO ₂	61.9	62.8	63.5	61.2	63.6
Al ₂ O ₃	19.5	19.0	19.2	19.9	18.8
FeO	-	0.12	0.36	0.32	0.82
CaO	0.43	0.38	0.33	0.56	0.10
BaO	3.34	1.88	0.36	3.69	0.94
Na ₂ O	0.67	0.52	0.78	0.80	0.53
K ₂ O	14.6	15.0	15.4	13.5	15.2
Total	100.44	99.70	99.93	99.97	99.99

Formula moles based on eight oxygens

Si	2.913	2.944	2.947	2.892	2.961
Al	1.079	1.050	1.051	1.107	1.032
Fe	-	0.004	0.013	0.012	0.031
Ca	0.021	0.018	0.015	0.027	0.004
Ba	0.061	0.034	0.005	0.068	0.016
Na	0.061	0.046	0.069	0.072	0.047
K	0.875	0.897	0.912	0.816	0.898
Total	5.008	4.994	5.012	4.994	4.990
An	2.2	1.9	1.5	3.0	0.4
Ab	6.4	4.8	6.9	7.9	5.0
Or	91.4	93.3	91.6	89.1	94.6

TABLE 4. Representative K-rich glass analyses from the 14303 VHK basalts.

PM No.	,245	,246	,249	,266	,275	,277
INAA No.	,244	,247	-	,266	,275	,277
SiO ₂	58.0	76.9	68.9	65.8	71.4	66.9
Al ₂ O ₃	19.0	13.6	15.6	18.4	14.4	17.9
FeO	7.09	0.69	0.53	0.36	0.49	0.25
CaO	1.08	0.77	0.46	0.52	0.58	0.02
BaO	1.76	0.30	0.90	0.73	0.64	0.12
Na ₂ O	0.89	0.45	0.60	0.66	0.57	0.45
K ₂ O	12.2	7.10	12.3	13.1	11.3	15.1
Total	100.02	99.81	99.29	99.57	99.38	100.74

TABLE 5. Representative olivine analyses from the 14303 basalts.

PM No. INAA No.	,245		,266		,277			
	,244		,266		,277			
	Mg-Rich	Fe-Rich	Inclusions in Plagioclase		Mg-Rich	Fe-Rich	Mg-Rich	Fe-Rich
SiO ₂	37.1	35.1	35.9	37.8	36.0	33.2	36.6	33.5
FeO	27.2	40.8	35.9	25.0	28.9	51.1	31.7	49.2
MnO	0.23	0.47	0.32	0.24	0.25	0.74	0.41	0.71
MgO	35.3	24.1	28.1	37.0	35.5	15.0	30.9	16.5
Total	99.83	100.47	100.22	100.04	100.65	100.04	99.61	99.91
<i>Formula moles based on four oxygens</i>								
Si	0.990	0.997	0.997	0.994	0.964	1.003	1.002	1.004
Fe	0.606	0.969	0.832	0.551	0.647	1.294	0.725	1.236
Mn	0.004	0.011	0.007	0.004	0.005	0.019	0.009	0.018
Mg	1.405	1.022	1.163	1.453	1.415	0.677	1.260	0.736
Total	3.006	2.999	2.999	3.002	3.032	2.993	2.995	2.994
Fo	69.9	51.3	58.3	72.5	68.6	34.3	63.5	37.3

2 while Mg# decreases from 79-60. At Mg# 60-56, the Al/Ti ratio decreases to 1. This suggests plagioclase crystallization occurred after the Mg# became lower than 60. Sample 14303,246 (Fig. 3b) contains pyroxenes exhibiting a small range in Mg# (67.5-70) or Al/Ti ratio (1.25-2.25). There is a possible positive correlation suggesting co-precipitation of pyroxene and plagioclase. Pyroxene compositions in the remaining two VHK basalts have constant Al/Ti ratios of approximately 2 (Figs. 3a and 3c), while Mg# decreases. This indicates possible plagioclase crystallization prior to pyroxene, as Al is reduced in pyroxene relative to other 14303 VHK clasts. Plagioclase phenocrysts are present in these samples.

Ilmenite is an interstitial phase that can form large (up to 0.75 mm in length), homogeneous masses (Table 7), some poikilitically enclosing plagioclase phenocrysts, as in ,245 (Fig. 1c). Also in ,245, ilmenite is associated with titaniferous chromite subsolidus reduction, and has a distinct composition (Mg# = 11.3) from the interstitial variety in this specimen (average Mg# = 17.7). Ilmenite also exhibits small ranges in composition in the other samples (Mg#: ,246 = 18.9-20.4; ,249 = 16.4-18.6; ,266 = 5.6-14.4; ,277 = 7.0-14.4). No ilmenite is present in ,275.

Members of the chromite-ulvöspinel series (Table 8) are present in ,245 ,266 and ,277. In ,245 they occur as two grains,

TABLE 6. Representative pyroxene analyses from the 14303 basalts.

PM No. INAA No.	,245			,246		,249		
	,244			,247		-		
	En	Pig	Aug	En	Aug	En	Pig	Aug
SiO ₂	52.8	51.6	50.2	53.1	51.4	51.8	51.8	50.7
TiO ₂	0.77	0.67	1.09	0.81	1.58	0.89	0.88	1.46
Al ₂ O ₃	1.73	0.80	1.63	0.85	1.60	1.06	0.81	1.70
Cr ₂ O ₃	0.64	0.24	0.48	0.30	0.31	0.41	0.32	0.48
FeO	15.3	23.1	13.4	19.2	10.1	21.3	20.4	10.4
MnO	0.20	0.34	0.25	0.25	0.19	0.35	0.32	0.21
MgO	25.9	18.9	14.2	24.1	15.2	22.5	20.1	15.6
CaO	2.31	4.64	18.2	1.72	20.0	1.70	6.01	19.6
Total	99.65	100.29	99.45	100.33	100.38	100.01	100.64	100.15
<i>Formula moles based on six oxygens</i>								
Si	1.923	1.951	1.909	1.952	1.913	1.933	1.937	1.900
Ti	0.020	0.019	0.030	0.021	0.043	0.024	0.024	0.042
Al	0.073	0.035	0.072	0.037	0.070	0.046	0.035	0.075
Cr	0.018	0.006	0.014	0.008	0.008	0.012	0.008	0.018
Fe	0.465	0.730	0.424	0.589	0.316	0.664	0.636	0.387
Mn	0.005	0.010	0.008	0.007	0.005	0.011	0.010	0.006
Mg	1.404	1.062	0.803	1.319	0.845	1.252	1.120	0.848
Ca	0.089	0.187	0.424	0.066	0.798	0.066	0.240	0.729
Total	3.999	4.000	4.003	4.000	3.999	4.008	4.010	4.004
En	71.8	53.7	40.8	66.8	43.2	63.2	56.1	43.2
Wo	4.5	9.4	37.7	3.2	40.7	3.3	12.0	37.1
Fs	23.7	36.9	21.5	29.8	16.1	33.5	31.9	19.7

TABLE 6. (continued)

PM No. INAA No.	,266			,275		,277	
	Pig	Aug	Ferro-Aug	Pig	Aug	Pig	Aug
SiO ₂	50.3	49.4	48.8	50.8	50.5	50.6	50.3
TiO ₂	0.71	1.36	1.46	0.85	1.33	0.89	1.48
Al ₂ O ₃	2.49	1.79	1.55	0.90	1.72	1.52	2.01
Cr ₂ O ₃	1.03	0.33	0.24	0.33	0.61	0.72	0.47
FeO	17.5	16.5	21.1	23.2	11.2	22.2	12.1
MnO	0.41	0.29	0.47	0.39	0.24	0.43	0.14
MgO	20.6	11.0	9.22	18.2	14.6	18.9	14.4
CaO	6.55	19.2	17.7	5.34	20.5	4.78	18.4
Total	99.59	99.87	100.54	99.98	100.70	100.04	99.30
<i>Formula moles based on six oxygens</i>							
Si	1.889	1.907	1.907	1.935	1.891	1.918	1.906
Ti	0.020	0.038	0.042	0.023	0.037	0.024	0.041
Al	0.108	0.080	0.071	0.040	0.076	0.068	0.089
Cr	0.029	0.009	0.007	0.009	0.018	0.021	0.013
Fe	0.545	0.532	0.688	0.740	0.351	0.703	0.383
Mn	0.012	0.009	0.007	0.009	0.018	0.021	0.013
Mg	1.148	0.633	0.536	1.032	0.816	1.066	0.814
Ca	0.262	0.796	0.741	0.218	0.821	0.193	0.745
Total	4.013	4.003	4.006	4.010	4.016	4.007	3.996
En	58.7	32.3	27.3	51.8	41.0	54.4	41.9
Wo	13.4	40.6	37.7	11.0	41.3	9.8	38.4
Fs	27.9	27.1	35.0	37.2	17.7	35.8	19.7

a euhedral 0.2×0.2 mm and a <0.1 mm diameter grain (see Fig. 1b). The larger grain is homogeneous [Mg# = 8.4–9.1; Cr/(Cr+Al) = 0.73–0.75] and is associated with ilmenite (see above) and native Fe, an assemblage typically indicative of a reduction reaction (*El Goresy et al.*, 1972). Only one analysis was possible from the smaller grain [Mg# = 16.1; Cr/(Cr+Al) = 0.67]. TiO₂ contents are higher in the larger grain. In ,266 and ,277, chromite-ulvöspinel are associated with pyroxene and olivine. Compositional heterogeneity is observed in the rare titaniferous chromites from ,266 [Mg# = 2.6–5.5; Cr/(Cr+Al) = 0.69–0.75; 27–35 wt % TiO₂] and in chromites from ,277 [Mg# = 9.0–23.6; Cr/(Cr+Al) = 0.60–0.79]. No

members of the chromite-ulvöspinel series are present in ,275, possibly a sampling problem. Zonation of these opaques to higher values for Ti, and lower Mg# and Cr/(Cr+Al) ratio toward the rims, is observed only in interstitial types and those associated with pyroxene. Chromites associated with olivine are relatively homogeneous. Such chromites formed early and

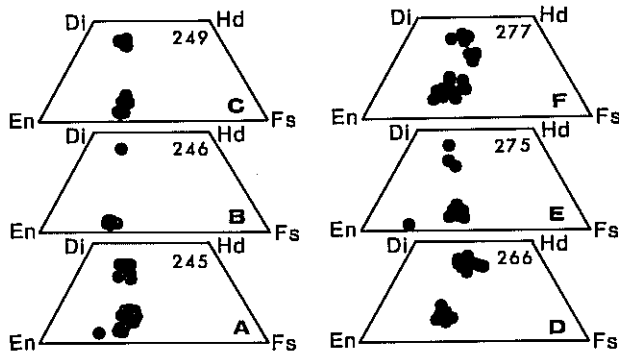


Fig. 2. Pyroxene compositions of the 14303 VHK basalts represented on a pyroxene quadrilateral. Generally there are two populations: Ca-poor and Ca-rich.

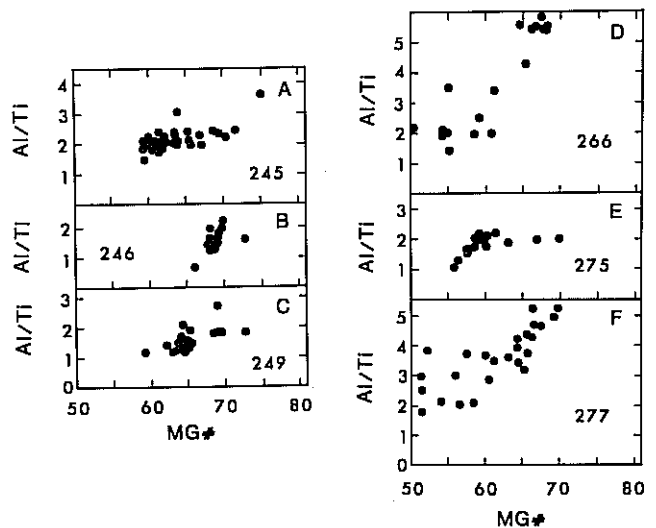


Fig. 3. Mg# versus Al/Ti ratio for each of the 14303 VHK basalt pyroxene populations. This figure serves to illustrate the effect of plagioclase crystallization (Al/Ti ratio) during the evolution of the VHK magma (decreasing Mg#). See text for discussion.

TABLE 7. Representative ilmenite analyses from the 14303 VHK basalts.

PM No.	,245	,246	,249	,266	,277
INAA No.	,244	,247	-	,266	,277
TiO ₂	55.6	53.8	56.3	55.3	53.6
Al ₂ O ₃	0.18	0.16	0.18	0.13	0.25
Cr ₂ O ₃	0.44	0.46	0.43	0.50	0.57
FeO	38.7	42.0	38.6	39.5	43.7
MgO	5.22	3.06	5.07	4.82	1.99
Total	100.14	99.48	100.58	100.25	100.11
<i>Formula moles based on three oxygens</i>					
Ti	1.005	1.000	1.013	1.004	0.997
Al	0.005	0.004	0.005	0.003	0.006
Cr	0.007	0.008	0.007	0.009	0.011
Fe	0.779	0.868	0.771	0.796	0.904
Mg	0.187	0.112	0.180	0.173	0.073
Total	1.983	1.992	1.976	1.985	1.991
Mg#	19.4	11.3	18.9	17.9	7.5

were encased in and protected by olivine, ensuring no further reaction with the remaining magma. As pyroxene crystallized after olivine and in some cases plagioclase, chromites associated with these minerals display zonation of the type described

TABLE 8. Representative chromite-ulvöspinel analyses from the 14303 VHK basalts.

PM No.	,245	,266	,277
INAA No.	,244	,266	,277
TiO ₂	24.7	11.2	26.7
Al ₂ O ₃	4.89	12.0	3.90
Cr ₂ O ₃	19.9	35.5	14.1
FeO	47.4	35.8	53.5
MgO	2.55	3.85	1.46
Total	100.46	98.65	99.66
<i>Formula moles based on four oxygens</i>			
Ti	0.648	0.291	0.725
Al	0.201	0.472	0.166
Cr	0.548	0.963	0.401
Fe	1.382	1.030	1.618
Mg	0.132	0.197	0.078
Total	2.934	2.965	2.987
Cr/(Cr+Al)	73.2	67.1	70.7
Mg#	8.7	16.1	4.6

TABLE 9. Ranges of Co and Ni in native Fe from the 14303 VHK basalts.

PM No./INAA No.	Co	Ni	Ni/Co
,245/,244	0.33-1.26	1.52-9.71	1.85-8.5
,246/,247	0.61	8.39	13.8
,249/ ---	0.31-0.51	3.16-4.83	7.94-11.1
,266/,266	0.01-0.10	0-0.95	0-39
,275/,275	0.12-0.80	0.71-6.85	2.25-10.3
,277/,277	0.03-1.27	0.07-2.84	0.11-6.07

above. These chromites continued to experience further interaction with the remaining magma (*El Goresy et al., 1972*).

Native Fe grains occur either enclosed in or interstitial to the other mineral phases. Grain sizes can reach up to 0.1 mm, but are usually <0.05 mm. These metal particles may be associated with ilmenite, probably the result of the subsolidus reduction of ulvöspinel (*El Goresy et al., 1972*). Native Fe compositions show a wide variation in Ni and Co contents (Table 9), but do not plot within the "meteorite field" (*Goldstein and Yakowitz, 1971*). Interstitial iron sulfide (troilite) is present in all 14303 VHK basalts and exhibits no significant compositional variation. Grain size is similar to the native Fe grains.

WHOLE ROCK CHEMISTRY

Analytical Techniques

Compositions of five 14303 VHK basalts were determined by INAA at Washington University using their standard procedure (*Lindstrom, 1984*). One clast (,249) was too small for INA analysis. All data were reduced employing the TEABAGS program of *Lindstrom and Korotev (1982)*. Relative uncertainties based on counting statistics at the one sigma level are: 1-2% for Fe, Na, Sc, Cr, Co, La, Sm, and Eu; 3-5% for Ca, Ce, Tb, Yb, Lu, Hf, Ta, and Th; 5-15% for Cs, Ba, Nd, and U; 15-25% for K, Sr, Ni, Rb, and Zr. All samples were analyzed for Ir and Au. Four samples contained Ir and Au abundances below the detection limit of 2 ppb, supporting a pristine origin for these basalts (*Warren and Wasson, 1979; Ryder et al., 1980; Warren et al., 1983b*). However, ,277 has a high Ni content (210 ppm) with Au and Ir abundances slightly higher than 2 ppb (3.9 and 2.7 ppb, respectively), indicative of meteoritic contamination.

Two VHK samples (,244 and ,247) were crushed and fused on a molybdenum strip in an atmosphere of argon. This permitted the major element composition (Table 10) of the whole rock to be determined on the quench glass by electron microprobe.

TABLE 10. Whole-rock compositions of the 14303 VHK basalts measured by INAA.

PM No.	,245	,246	,266	,275,	277
INAA No.	,244	,247	,266	,275	,277
Weight (mg)	24.4	13.6	15.2	20.9	22.4
	P	P	I	I	I
SiO ₂	48.7	48.9	na	na	na
TiO ₂	1.61	1.70	na	na	na
Al ₂ O ₃	18.2	13.4	na	na	na
FeO	9.55	13.6	16.8	9.90	12.9
MgO	8.27	9.68	na	na	na
CaO	12.3	10.4	10.5	11.0	9.9
Na ₂ O	0.45	0.55	0.49	0.72	0.64
K ₂ O	<0.75*	1.05	1.30	1.10	0.86
Sc	30.0	46.0	57.8	20.8	37.9
Cr	1777	2595	3350	1014	2720
Co	19.4	31.8	31.6	15.3	34.9
Ni	50	150	110	65	210
Rb	10	39	37	38	23
Sr	155	125	<100	160	92
Cs	0.20	1.41	0.89	1.75	0.99
Ba	300	800	587	930	2720
La	18.1	41.3	8.51	37.1	52.0
Ce	47.2	109	22.7	94.0	127
Nd	27.0	60.0	12.0	54.0	79.0
Sm	9.26	19.3	4.82	16.3	24.4
Eu	1.62	1.56	0.94	1.96	1.90
Tb	2.13	4.14	1.12	3.65	4.83
Yb	6.91	13.7	4.49	16.3	17.5
Lu	1.05	2.09	0.71	2.60	2.45
Zr	245	500	nd	550	700
Hf	6.00	13.0	2.82	14.0	17.7
Ta	0.73	1.81	0.59	1.65	2.08
Th	2.20	7.97	1.15	8.27	9.76
U	0.65	2.37	0.55	2.40	3.35
Ir(ppb)	nd	nd	nd	nd	3.9
Au(ppb)	<3	<3	<5	<4	2.7

na = not analyzed.

nd = not detected.

P= major elements by probe analysis of fused glass.

I = all elements by INAA.

*Analysis from INAA.

Results

Whole rock compositions are presented in Table 10. The major element composition of ,247 (PM = ,246) determined by the fusion method is comparable with those major elements analyzed by INAA. However, although ,244 has similar results from INAA and the fusion method for Ca and Na, the absolute determination of K by the fusion method (0.23 wt % K₂O) is within the mare basalt range, rather than VHK. We consider 0.23 wt % K₂O too low to account for the interstitial high-K glass (Tables 1 and 4) in this sample. This highlights the problem of sample size and representative sampling, especially as the INAA sample masses are particularly low (e.g., 13.6-24.4 mg). It would seem apparent that 14303,244 used for the INA and EMP fusion analyses did not sufficiently sample the high-K glass witnessed in the companion probe mount (,245).

An approximate K₂O value may be determined by modal reconstruction, using the probe mount ,245. By employing this method, 0.75 wt % may be taken as the maximum K₂O abundance in PM ,245 (,244). Abundances of Na and Ca are similar to those in HA basalts (Shervais *et al.*, 1985b; Dickinson *et al.*, 1985; Neal *et al.*, 1987a) of 0.48-0.72 and 9.9-12.3 wt %, respectively. Iron concentrations in the 14303 VHK basalts (9.9-16.8 wt % FeO) overlap and are lower than in mare basalts. The low Fe and high Al in 244 indicate that this sample is plagioclase-rich relative to other VHK basalts. There is a much higher concentration of K in the 14303 samples (0.75-1.30 wt %) than in mare basalts. These major element analyses are similar to other previously reported VHK basalts (Shervais *et al.*, 1985b; Goodrich *et al.*, 1986; Warren *et al.*, 1986), except for the high Al content of ,244 (18.2 wt %). The high K₂O contents of the parental magmas account for the presence in these basalts of K-rich glass in all specimens

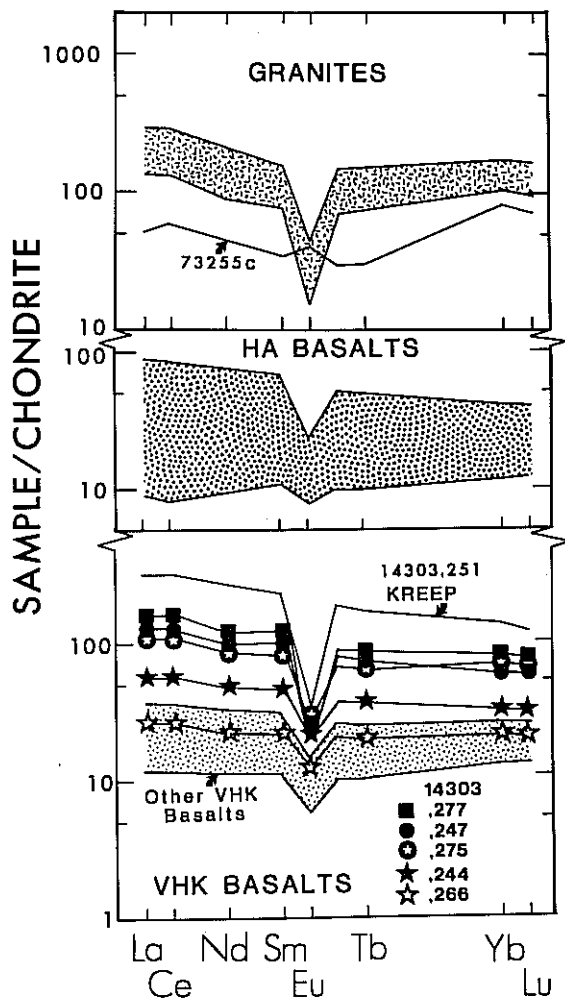


Fig. 4. The REE profiles of the 14303 VHK basalts are compared to others previously reported (stippled area: data of *Sbervais et al.*, 1985b; *Goodrich et al.*, 1986; *Warren et al.*, 1986) and a KREEP basalt also from breccia 14303. Shown for comparison are the entire range of Apollo 14 HA mare basalts (*Dickinson et al.*, 1985; *Sbervais et al.*, 1985a; *Neal et al.*, 1987a) and granite compositions (*Blanchard and Budabn*, 1979; *Warren et al.*, 1983c; *Salpas et al.*, 1985).

and K-feldspar in all but ,244 (,245). This sample [,244 (,245)] has lower K_2O than other 14303 VHK samples reflecting the lack of K-feldspar.

The trace element abundances presented here extend the ranges previously reported for VHK basalts. These elements are sensitive to the many igneous processes that operate during magma evolution. For ease of presentation, the trace elements will be discussed as groups of elements with similar physico-chemical affinities. The 14303 samples will be compared and contrasted with those previously reported (*Sbervais et al.*, 1985b; *Goodrich et al.*, 1986; *Warren et al.*, 1986), as well as with ordinary Apollo 14 mare basalts (*Dickinson et al.*, 1985; *Neal et al.*, 1987a; *Sbervais et al.*, 1985a).

Rare earth elements (REE). The REE contents of the 14303 VHK basalts exhibit a wide range of abundances (Table

6) that overlap those of mare and other VHK basalts and extend to much higher values (Fig. 4). Samples containing the greatest REE contents are LREE enriched, showing a similarity to KREEP (Fig. 4), being distinguished from KREEP on the basis of K/La ratio (except ,277). All 14303 samples have the characteristic negative Eu anomaly and there is a slight enrichment of the LREE over the HREE. REE abundances are within the ranges reported for Apollo 14 HA basalts (Fig. 4).

Compatible elements: Sc, Cr, Co, Ni. The five 14303 VHK basalts have a wide range in compatible element abundances. Abundances of Sc (20.8–57.8 ppm), Cr (1014–3350 ppm), and Co (15.3–34.9 ppm) overlap but are generally lower than abundances in mare basalts and previously reported VHK basalts. However, nickel abundances (50–210 ppm) overlap and are higher than mare basalts and previously reported VHK compositions. If ,277 is omitted, the range is reduced to 50–150 ppm Ni, which is comparable with other VHK basalts. In fact, the Ni/Co ratio of ,277 is the highest in any reported VHK basalt (6.0) and is similar to the Ni/Co ratios of Apollo 15 impact melts reported by *Ryder and Spudis* (1987). However, ,247 and ,275 also fall within this range (4.7 and 4.2, respectively). Therefore, it is pertinent to compare the abundances of Ir and Au in these samples to determine whether any significant meteoritic component is present (i.e., origin as an impact melt). Indeed, sample ,277 contains the highest amounts of Ir (3.9 ppb) and Au (2.7 ppb). Therefore, we conclude that 14303,277 contains a meteoritic component and is probably the crystallized product of an impact melt rather than a pristine VHK basalt. This will be highlighted in the discussion below.

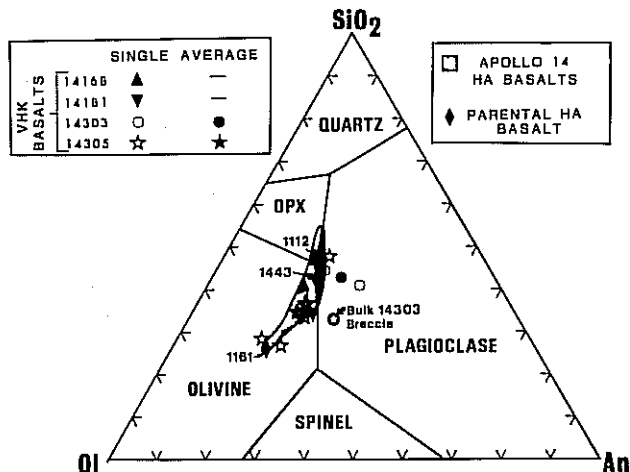


Fig. 5. Representation of VHK basalt data on a SiO_2 -Ol-Plag pseudoternary (after *Walker et al.*, 1972). These are compared with all Apollo 14 HA mare basalts (*Dickinson et al.*, 1985; *Sbervais et al.*, 1985a; *Neal et al.*, 1987a). Generally, the VHK basalts fall along the inferred crystallization path of the HA compositions. Phase boundaries are calculated for an Fe/(Fe+Mg) ratio of 0.6, the magma composition upon just encountering the Ol-Plag cotectic (composition calculated using the method of *Longhi*, 1977). Note that the two 14303 basalts plotted bear no similarity to the bulk rock 14303 breccia composition (data of *Brunfelt et al.*, 1972). The three HA magma compositions, taken as parental to VHK basalts, are also shown.

TABLE 11a. Crystal/liquid partition coefficients.

	Olivine	Pyroxene	Plagioclase	Chromite	Ilmenite
K	0.0068	0.014	0.17	0	0
Ba	0.03	0.013	0.686	0.005	0.005
Hf	0.04	0.063	0.05	0.38	1.817
Th	0.03	0.13	0.05	0.55	0.55
La	(0.0001)	(0.012)	0.051	0.029	0.029
Ce	0.0001	0.038	0.037	0.038	0.038
Sm	0.0006	0.054	0.022	0.053	0.053
Eu	0.0004	0.1	1.22	0.02	0.02
Yb	0.02	0.671	0.012	0.39	0.39
Lu	(0.02)	0.838	0.011	0.47	0.47

Brackets indicate estimated partition coefficient.

Chromite REE partition coefficients taken as those for ilmenite.

References: *Arb and Hanson (1975)*; *Binder (1982)*; *Drake and Weill (1975)*; *Haskin and Korotev (1977)*; *Irving and Frey (1984)*; *McKay et al. (1986)*; *Schnetzler and Philpotts (1970)*; *Villemant et al. (1981)*.

TABLE 11b. Modeling parameters

	Parental Magmas			Assimilated Granite	
	,1161	,1443	,1112	73255c	Average Granite
K	564	747	1826	62665	58864
Ba	32	130	216	5470	4490
Hf	1.78	5.43	11.5	16.0	15.4
Th	0.20	1.50	2.90	9.50	42.3
La	2.89	13.5	30.6	20.3	50.7
Ce	8.40	35.0	82.9	50.0	123
Sm	2.11	7.59	15.3	6.74	16.7
Eu	0.56	1.12	1.67	2.71	2.52
Yb	2.89	6.33	9.72	10.3	24.7
Lu	0.47	0.91	1.33	1.50	3.71

References: *Sbervais et al. (1985a)*; *Neal et al. (1987a)*; *Blanchard and Budahn (1979)*; *Warren et al. (1983c)*; *Salpas et al. (1985)*.

Large ion lithophile (LIL) elements: Rb, Sr, Cs, Ba. The LIL elements exhibit a wide range of abundances (Rb = 10-39 ppm; Sr = 92-160 ppm; Cs = 0.2-1.75 ppm; Ba = 300-2720 ppm). All extend the upper ranges of previously reported VHK compositions to higher values. Sample 14303,277 contains anomalously high Ba abundances (2720 ppm) that, if omitted, reduce the Ba range to 300-930 ppm, comparable with other VHK basalts. Rubidium and Cs abundances in the 14303 samples are higher than and overlap those of the mare basalts, whereas Sr is within the mare basalt range. However, Ba is distinctly higher than any mare basalt composition, even if ,277 is omitted.

High field strength (HFS) elements: Zr, Hf, Ta, Tb, U. As with the element groups discussed above, the HFS element abundances exhibit wide variances (Zr = 245-700 ppm; Hf = 2.82-17.7 ppm; Ta = 0.59-2.08 ppm; Th = 1.15-9.76 ppm; U = 0.55-3.35 ppm). Sample 14303,277 contains the greatest abundances of these elements, which are similar to abundances present in KREEP (e.g., *Warren et al., 1983d*). However, even if sample ,277 is omitted, the 14303 VHK basalts still have HFS abundances that are higher than and overlap the compositions of mare and previously reported VHK basalts.

MODELING

Introduction

The analysis and recognition of very high potassium (VHK) basalts (*Warner et al., 1980*; *Sbervais et al., 1985b*) presented a highly significant rock type whose origin will be indicative of petrologic processes that have operated at the Apollo 14 site. Several authors (e.g., *Sbervais et al., 1985b*; *Warren et al., 1986*) have favored the theory of granite assimilation versus a metasomatized source for VHK basalt petrogenesis. However, it is recognized that this model is not complete; the high K/Th and K/U ratios of the VHK basalts cannot be generated by simple mass balance granite assimilation (e.g., *Sbervais et al., 1985b*; *Warren et al., 1986*; *Sbib et al., 1987*).

In this paper, we present a combined Assimilation and Fractional Crystallization (AFC) model for VHK basalt petrogenesis. Our model is designed to encompass all reported VHK compositions into one dynamic process that can explain both the wide range of elemental abundances and the rarity of VHK compositions at the lunar surface.

TABLE 12. Modeling results (ppm).

Parent/Granite	.1161/73255c				.1161/Av. Granite			
F Value	0.95	0.90	0.85	0.80	0.95	0.90	0.85	0.80
K	3890	7584	11709	16347	3690	7162	11039	15398
Ba	321	641	998	1398	312	614	898	1298
Hf	2.70	3.71	4.83	6.08	2.67	3.64	4.73	5.94
Th	0.71	1.26	1.88	2.57	2.43	4.88	7.59	10.6
La	4.11	5.46	6.98	8.68	5.71	8.84	12.3	16.3
Ce	11.8	14.9	18.7	23.0	15.3	23.0	31.6	41.3
Sm	2.57	3.09	3.67	4.31	3.10	4.20	5.42	6.80
Eu	0.73	0.92	1.14	1.38	0.72	0.90	1.10	1.33
Yb	3.57	4.31	5.14	6.06	4.32	5.90	7.66	9.62
Lu	0.57	0.68	0.80	0.94	0.69	0.92	1.19	1.48
Parent/Granite	.1443/73255c				.1443/Av. Granite			
F Value	0.95	0.90	0.85	0.80	0.95	0.90	0.85	0.80
K	4063	7561	11316	15476	3863	7154	10684	14595
Ba	415	711	1027	1371	364	608	868	1151
Hf	6.51	7.57	8.65	9.82	6.48	7.51	8.55	9.68
Th	2.06	2.64	3.25	3.93	3.78	6.16	8.67	11.4
La	15.2	17.0	19.0	21.2	16.8	20.3	24.1	28.3
Ce	39.4	44.2	49.1	54.6	43.2	52.1	61.4	71.8
Sm	8.33	9.10	9.92	10.8	8.85	10.2	11.6	13.2
Eu	1.25	1.39	1.54	1.71	1.24	1.36	1.51	1.66
Yb	7.17	7.87	8.46	9.09	7.92	9.39	10.8	12.2
Lu	1.03	1.12	1.19	1.27	1.15	1.36	1.55	1.74
Parent/Granite	.1112/73255c				.1112/Av. Granite			
F Value	0.95	0.90	0.85	0.80	0.95	0.90	0.85	0.80
K	5198	8920	13054	17671	4999	8503	12392	16738
Ba	507	823	1169	1547	456	717	1002	1314
Hf	12.7	13.9	15.3	16.7	12.6	13.8	15.2	16.6
Th	3.50	4.16	4.89	5.69	5.22	7.75	10.5	13.6
La	33.2	36.1	39.3	42.9	34.8	39.4	44.6	50.4
Ce	89.6	96.9	105	114	93.4	105	118	132
Sm	16.4	17.6	18.9	20.4	16.9	18.7	20.7	22.9
Eu	1.82	1.98	2.16	2.34	1.81	1.96	2.12	2.30
Yb	10.3	10.9	11.6	12.3	11.0	12.5	13.9	15.5
Lu	1.40	1.47	1.55	1.63	1.51	1.70	1.91	2.12

Modeling Systematics

In the proposed model, granite is inferred to be an assimilated component by an Apollo 14 high-Al (HA) mare basalt magma. Although treatment of assimilation as a mass balance or bulk mixing problem may be a good first approximation, any assimilation will be accompanied by some magma crystallization (DePaolo, 1981). This is a more plausible approach than simple mixing of granite and HA basalt (Sibb et al., 1987). The composition of the crystallizing phases will evolve as this process proceeds. We have attempted, where possible, to account for these evolving compositions within our major element modeling in order to represent a realistic situation. The proportions and nature of fractionating phases can be calculated from phase equilibria. These results can then be applied to the trace elements. Such an approach is critical

for consistency between major and trace element modeling and is essential in the development of any model for magma petrogenesis.

Major elements. A major constraint in any petrologic modeling is the phase equilibria applicable to that particular melt, and numerous experimental investigations of mare basalt liquids have been performed (e.g., Walker et al., 1972; Kesson, 1975). It was determined that the basaltic phase relations could most readily be explained by consideration of the SiO₂-O1-An pseudoternary system (often referred to as the "Walker Diagram"). We feel this is a feasible approach as the diopside component is low (approximately 10% in each case), which will impart insignificant errors in the overall modeling. All reported major element compositions of VHK basalts are represented on such a Walker diagram in Fig. 5 along with the range in Apollo 14 HA basalts. The petrogenesis of the

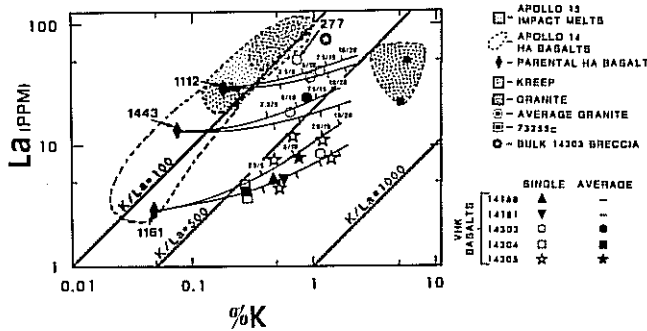


Fig. 6. K% versus La (ppm) to demonstrate the role of granite assimilation in the petrogenesis of VHK basalts. AFC paths are calculated from the three HA magmas (these span the range of Apollo 14 HA basalts), with the upper and lower paths in each case representing average granite and 73255c as the respective assimilants. Tick marks represent increments of 5% fractional crystallization (2.5% granite assimilation). These same increments will be repeated, but without numbers, in subsequent diagrams. Note that 14303,277 cannot be generated by any of these paths and has similar K/La ratios to the bulk rock 14303 breccia.

HA major element compositions by fractional crystallization (Neal *et al.*, 1987a) can be extended to the VHK basalts because of the similarity of their major element abundances. The phase boundaries (e.g., cotectics) in this system have been shown to be particularly sensitive to the Fe/(Fe+Mg) ratio of the system (Walker *et al.*, 1973; Longhi, 1977). As such, the phase boundaries are drawn for the Fe/(Fe+Mg) of the system just as the evolving melt encounters the Ol-Plag cotectic (Fe/(Fe+Mg) \cong 0.6). The major elements are modeled by fractional crystallization only, as the major elements are effectively controlled by the fractionating phases (DePaolo, 1981). However, with a high proportion of granite assimilation, this may have an effect on the major element modeling, probably slightly increasing the proportion of plagioclase fractionation. We feel that this will not significantly affect the overall results of our fractional crystallization modeling.

Trace elements. The process of assimilation will have a profound effect on the trace elements, and thus these elements cannot be modeled by fractional crystallization alone. We have modeled the trace elements by combined assimilation and fractional crystallization, using equation (6a) of DePaolo (1981)

$$C_m/C_m^0 = F^{-z} + \left(\frac{r}{r-1} \right) \left(\frac{C_a}{zC_m^0} \right) (1 - F^z)$$

where r = mass assimilated/mass crystallized; z = $r+D-1/r-1$; D = bulk distribution coefficient; C_m^0 = concentration of element in the parental magma; C_m = concentration of element in the residual magma; C_a = concentration of element in the assimilated component; F = proportion of liquid remaining.

The inferred ratio of the mass assimilated to the mass crystallized (r value) is relatively high (0.5). This value

represents a realistic figure of a high-temperature basaltic magma assimilating a granitic component of lower melting point (e.g., Watson, 1982).

Components. As has been reported by Neal *et al.* (1987a), HA mare basalts show a wide range of compositions at the Apollo 14 site. This compositional range is due to evolution of a primitive HA magma by combined assimilation and fractional crystallization with KREEP. Therefore, in order to represent this wide range of HA basalts, we have chosen three compositions as our parental VHK magmas (14321,1161 of Sbervais *et al.*, 1985a; 14321,1443 and 14321,1112 of Neal *et al.*, 1987a). These compositions span the range of Apollo 14 HA mare basalts (see Fig. 5). Sample ,1161 plots within the olivine field; ,1443 falls on the Ol-Plag cotectic; and ,1112 falls on the Ol-Opx-Plag peritectic reaction point.

The proportions of fractionating phases for the three HA parental magmas have been calculated by the Lever Rule from Fig. 5. If 14321,1161 produced all reported VHK compositions, it would have to undergo approximately 60% fractional crystallization. During the first 25% crystallization, olivine (90%) + chromite (10%) are the only phases to fractionate (Walker *et al.*, 1972), at which point the Ol-Plag cotectic is encountered. During 25% to 45% crystallization, plagioclase (50%) + olivine (40%) + chromite (10%) are fractionated, after which the Ol-Opx-Plag peritectic is encountered. It is envisaged that all fractionating phases are effectively removed from the system; therefore, olivine does not undergo any back-reaction. Between 45% and 60% crystallization of ,1161, orthopyroxene (60%) + plagioclase (30%) + ilmenite (10%) are fractionated.

If composition 14321,1443 is taken as parental to the VHK basalts, it would have to undergo approximately 25% fractional crystallization. During the first 7% crystallization, plagioclase (50%) + olivine (40%) + chromite (10%) would fractionate. At this point, the Ol-Opx-Plag peritectic is encountered, and orthopyroxene replaces olivine on the liquidus. From 7% to 25% crystallization, orthopyroxene (60%) + plagioclase (30%) + ilmenite (10%) are fractionated.

If composition 14321,1112 is taken as parental to the VHK basalts, it would only be required to undergo between 10-15% fractional crystallization. This composition cannot be parental to all VHK basalts. As ,1112 lies approximately on the Ol-Opx-Plag peritectic, orthopyroxene (60%) + plagioclase (30%) + ilmenite (10%) would be the only fractionating phases.

The proportions of fractionating mineral phases are the same as in Apollo 14 mare basalt evolution by AFC with KREEP (Neal *et al.*, 1987a), indicating the similarity in petrogeneses.

Reported granite compositions demonstrate that although these tend to be heavily enriched in the LIL and HFS elements, a wide range in compositions exists (e.g., Warren *et al.*, 1983c). For our modeling purposes, we have taken: (1) an average of seven granite compositions (five from Warren *et al.*, 1983c and two "new" samples from 14305 of Salpas *et al.*, 1985); and (2) the composition of 73255c (Blanchard and Budahn, 1979; Warren *et al.*, 1983c). The majority of granite compositions approximate that of the average, except for 73225c. This sample generally has the lowest granite trace element abundances. A peculiar feature of granite 14305 is

the positive Eu anomaly rather than the usual negative one. Therefore, use of an average composition will best represent all other compositions, apart from 73255c. Incorporation of these two granite compositions in our modeling should be more representative than a single, skewed average composition.

Effects of short-range unmixing. The small sample sizes analyzed will undoubtedly induce errors due to unrepresentative sampling. The effects of these errors are attributable to short-range unmixing (Haskin and Korotev, 1977; Lindstrom and Haskin, 1978) of a solidifying magma. This process is similar to fractional crystallization, except there is no large-scale separation of crystallized products and residual liquid. Short-range unmixing deals with centimeter-sized inhomogeneities in materials that may be homogeneous on a meter scale (Lindstrom and Haskin, 1978). This may explain the plagioclase-rich nature of 14303,245 relative to 14303,246. In order to minimize the possible effects of short-range unmixing, average compositions have been calculated in Fig. 5 (and succeeding figures) for VHK compositions from the 14303, 14304, and 14305 breccias. Single analyses for VHK basalts from 14168 and 14181 are also shown. However, short-range unmixing alone cannot account for the wide range in major and especially trace element abundances observed in the VHK basalts.

Major element modeling. We have not presented quantitative modeling on Fig. 5, as it is envisaged that *one parental HA magma is not responsible for the array of VHK compositions*. However, it is demonstrable that a large proportion of olivine fractionation is required in order to generate these basalts if 14321,1161 is taken as the parental composition [e.g., 14303,246 may be generated from ,1161 by 25% crystallization of olivine (90%) + chromite (10%), followed by 20% crystallization of olivine (40%) + plagioclase (50%) + chromite (10%)]. In order to recreate realistic crystallizing conditions, the Fo content of fractionating olivine was calculated iteratively in crystallization increments of 2% using the Mg/Fe ratio of the resultant liquid to calculate the Fo content of the crystallizing olivine (similar to Longhi, 1977). With ,1161 as the parental composition, olivine remains on the liquidus approximately until 45% is crystallized. This yields a range in the Fo content from 80 to 60 and may explain the upper range observed in VHK basalts. But there are basalts with olivines of various Fo contents. The lower range of olivine Fo contents is considered to be a late-stage phenomenon (Sbervais et al., 1985b). The simplified assumption of complete olivine removal (i.e., no back-reaction) during crystallization may not be totally correct.

Comparison of the major element data (where available) on a Walker diagram (Fig. 5) illustrates that, in general, the VHK basalts have similar compositions to the Apollo 14 mare basalts. Only 14303,247 plots in the Plag field, reflecting the feldspar-rich nature of this sample. The VHK basalt major element compositions display a similar crystallization path to that of Apollo 14 HA mare basalts. Two 14305 VHK compositions reported by Sbervais et al. (1985b) are primitive (14305,304 and ,384), similar to the parental composition 14321,1161. Modeling of the major elements in this way is feasible, even though we also envisage assimilation of a granitic component (see section on Modeling Systematics).

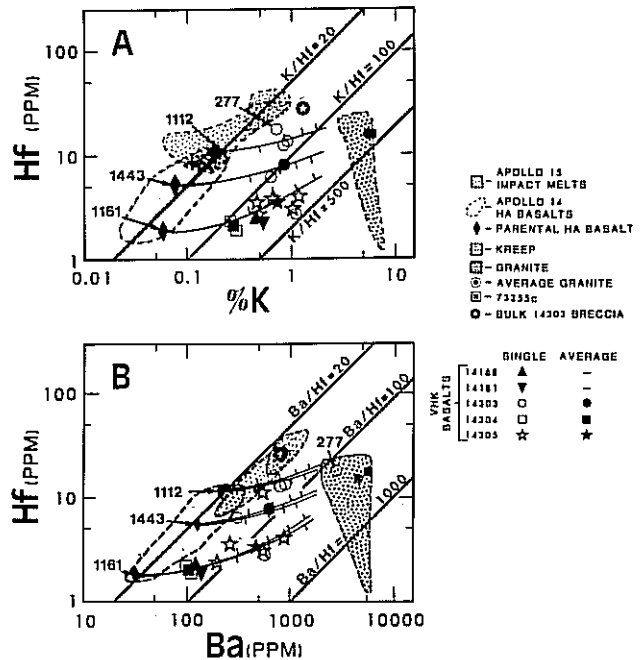


Fig. 7. Illustrations of the enrichment of K and Ba in VHK basalts due to the effect of granite assimilation. (a) K% versus Hf (ppm); AFC paths are calculated from the three parental HA magmas. As average granite and 73255c have similar K and Hf abundances, the calculated paths plot on top of each other. Note that 14303,277 cannot be generated by these AFC paths and has similar K/Hf ratios to the bulk rock 14303 breccia. (b) Ba (ppm) versus Hf (ppm); VHK basalts generated by ,1161 and 73255c can be generated in the same order as in (a) along calculated AFC paths, but amounts are reduced. This is due to the high Ba abundance in 73255c. The upper and lower paths in each case represent 73255c and average granite as the respective assimilants. Note that 14303,277 falls within the granite field on this diagram, due to elevated Ba abundance.

Trace Element Modeling

We have attempted to model the critical elements involved in VHK basalt petrogenesis, namely K, Ba, Hf, Th, and the REE. We have not modeled U because of the incomplete data set for U in the VHK basalt and granite suites and the lack of accurately determined crystal-liquid partition coefficients. Three parental magma compositions are again taken as 14321,1161, 1443 and ,1112. Crystal-liquid partition coefficients and parameters used are presented in Table 11. Results obtained are presented in Table 12. In Figs. 6-8, all VHK basalt data are plotted with (1) granite (Warren et al., 1983c; Salpas et al., 1985), (2) KREEP (Vaniman and Papike, 1980; Warren et al., 1983d), (3) Apollo 14 HA mare basalts (Neal et al., 1987a; Dickinson et al., 1985; Sbervais et al., 1985a), (4) the bulk 14303 breccia composition (Brunfelt et al., 1972), and (5) Apollo 15 impact melt compositions (Ryder and Spudis, 1987). This approach is designed to demonstrate the petrogenesis of VHK basalts from assimilation of lunar granite by a HA mare basalt, rather than from an impact melt.

Figure 6 illustrates the familiar plot of K versus La for lunar

granite, KREEP, and HA basalts. This diagram demonstrates that KREEP and Apollo 14 mare basalts have similar K/La ratios (50-100), but VHK basalts diverge from this trend, removed somewhat toward granite (K/La = 500-750). The Apollo 15 impact melts have similar K/La ratios to mare basalts and KREEP, unlike the VHK basalts, with the possible exception of 14303,277. AFC paths have been calculated from the three parental magmas defined above, using average granite and 73255c as assimilants. It is obvious that it is not possible to generate all VHK data using one parent and one granite composition.

In Fig. 6, we have averaged the VHK data according to the breccia in which they were identified (cf. Fig. 5). As depicted in Fig. 6, the 14304 VHK basalts can be generated from the parental basalt 14321,1161 by approximately 4% fractional crystallization and 2% assimilation of granite 73255c. The 14305 VHK basalts can be generated from the parental basalt 14321,1161 by 10% fractional crystallization and 5% assimilation of the average granite composition. It is possible that both of these averaged compositions can be generated by either the average granite or 73255c assimilants. *Shih et al.* (1986, 1987) performed mass balance mixing calculations and arrived at the same amounts of granite assimilation for 14304 and 14305 VHK basalts as calculated by our AFC considerations. When the amounts of assimilation and fractional crystallization are small, the AFC process can be approximated by more simple mass balance calculations. However, it is important to consider crystallization from the melt concomitant with assimilation of the granite. We insist that these AFC calculations represent a more realistic approach to the natural situation.

The VHK compositions described by *Warren et al.* (1986) and *Sbervais et al.* (1985b) from breccias 14181 and 14168 also fall along the AFC path between 14321,1161 and 73255c.

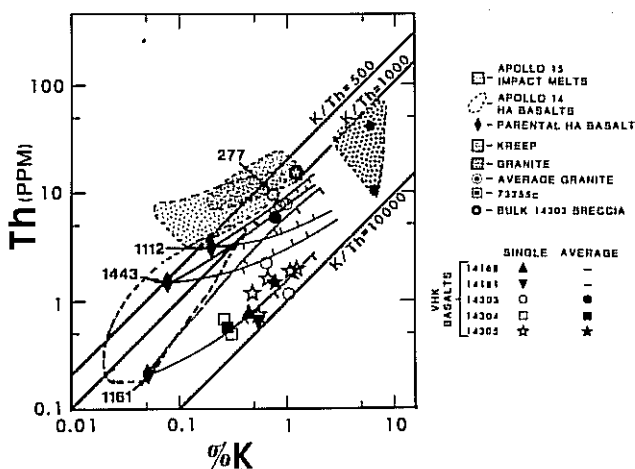


Fig. 8. K% versus Th (ppm); AFC paths are calculated as in Figs. 6 and 7. The proportions of fractional crystallization and granite assimilation are the same as in Figs. 6 and 7. The upper and lower paths in each case represent average granite and 73255c as the respective assimilants. Note that 14303,277 falls within the impact melt field on this diagram and has a similar K/Th ratio to the bulk rock 14303 breccia.

14168 is generated after 6% fractional crystallization (3% granite assimilation) and 14181 is generated after 7% fractional crystallization (3.5% granite assimilation). There is a progression of VHK compositions along this AFC path (i.e., increasing granite component) from 14304, through 14168 and 14181, to 14305.

The average 14303 VHK composition cannot be generated by parental basalt 14321,1161 (recall that the average was calculated without including ,277 since this is considered to be an impact melt). The average 14303 VHK basalt can be generated by approximately 11.5% fractional crystallization of parental basalt 14321,1443, with 5.75% assimilation of average granite. Those individual 14303 VHK basalts with lower K/La ratios can only be generated by AFC between parental basalt 14321,1112 and average granite. Note that 14303,277 cannot be generated by this model.

Figure 7a presents K versus Hf, and Fig. 7b depicts Ba versus Hf. These plots serve to illustrate the similarity between the behaviour of K and Ba in VHK basalt petrogenesis. Mare basalts, KREEP, and impact melts have similar K/Hf and Ba/Hf ratios (10-20 and 20-50, respectively), with VHK compositions removed toward granite, which has elevated K/Hf and Ba/Hf ratios (200-1000 and 200-1200, respectively). The proportions of granite assimilation and fractional crystallization are the same as in Fig. 6 in order to generate the average VHK basalt compositions in Fig. 7a (K versus Hf) for 14168, 14181, 14303, 14304, and 14305. For Ba against Hf (Fig. 7b), these proportions are reduced for VHK basalts generated by parent magma ,1161 and granite 73255c. This is necessary because although most trace elements are less abundant in 73255c relative to average granite, Ba abundance is higher (5470 ppm). The average 14303 VHK basalt is generated by the same proportion of fractional crystallization of ,1443 and assimilation of average granite as in Fig. 6. However, the same general progression along the AFC path between 14321,1161 and 73255c is maintained, described in Fig. 6 for 14304, 14168, 14181, and 14305 compositions. In both Figs. 7a and 7b, those individual 14303 VHK basalts with lower K/Hf and Ba/Hf can only be generated by AFC between 14321,1112 and average granite. Note here again, as in Fig. 6 14303,277 cannot be generated on either plot by our model, which suggests an origin different from that proposed for other VHK compositions.

Elements that are problematic from a mass balance point of view in VHK basalt petrogenesis are U and Th (see above). We have not modeled U due to the lack of published crystal/liquid partition coefficients. However, it is considered that U and Th should behave in a similar manner, implying that the AFC paths for U will approximate the results obtained for Th. Partition coefficients for Th are sparse, and we have conducted our modeling using the few we could find in the literature.

It has been considered that K/Th ratios in VHK basalts are too high to be the result of bulk granite assimilation (*Warren et al.*, 1986), but may be generated by selective assimilation of granitic feldspars only (*Sbervais et al.*, 1985b; *Shih et al.*, 1987). In Fig. 8, K is plotted against Th, demonstrating that Apollo 14 HA mare basalts, KREEP, and Apollo 15 impact melts have similar K/Th ratios of 500-1000. The majority of individual VHK samples and the average 14304 and 14305 compositions can be generated by AFC between parental basalt 14321,1161

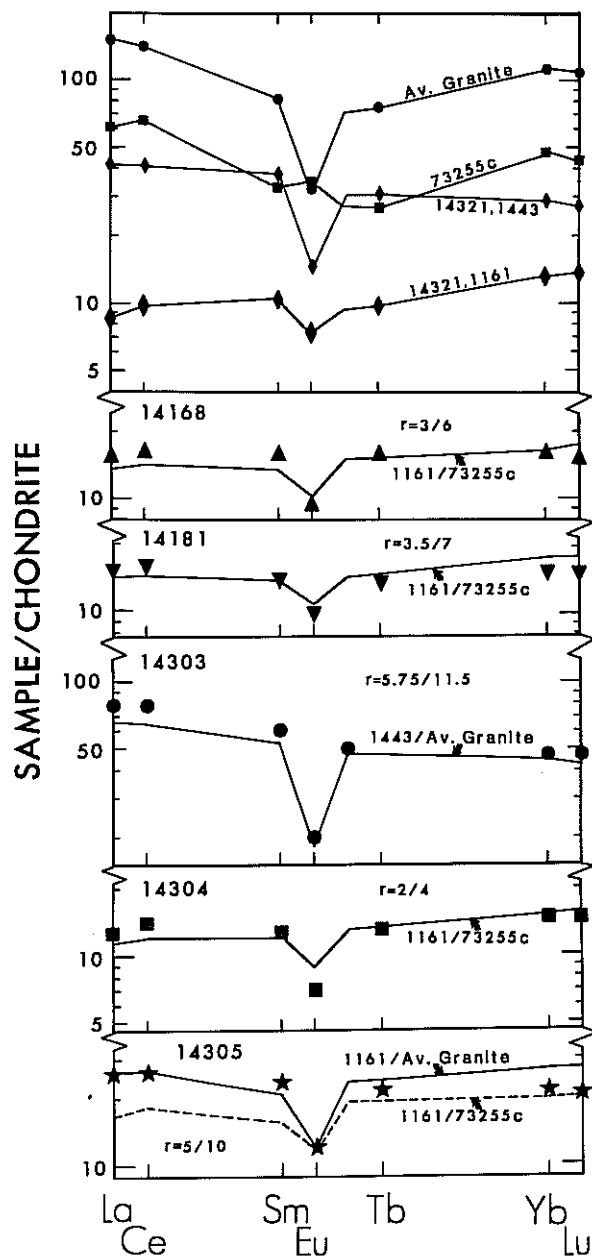


Fig. 9. REE modeling diagrams. The proportions of fractional crystallization and granite assimilation, as well as the composition of the parental HA magma and assimilated granite, have been determined in Figs. 5-8. Average compositions are modeled for 14303, 14304, and 14305 VHK basalts, and the REE profiles of the components used are shown. Symbols represent the actual reported compositions, and the solid lines represent the modeling results. The "r" values quoted represent the "mass assimilated/mass crystallized."

and the granite 73255c. The average 14304 VHK basalt is generated by 4% fractional crystallization (2% granite assimilation). 14181 and 14168 also fall on this AFC path, being generated by 10% fractional crystallization (5% granite assimilation), whereas the average 14305 VHK basalt is

generated by 7% and 6% fractional crystallization (3.5% and 3% granite assimilation), respectively. Likewise, the average 14303 VHK basalt is generated by 11.5% fractional crystallization of 14321,1443 (5.75% assimilation of average granite). These values were also obtained in Fig. 6 and 7a. Our results demonstrate that the main problem in VHK basalt petrogenesis, of generating K/Th (and K/U) ratios, is overcome by our realistic AFC modeling approach and by the more detailed examination of published granite compositions. Note once again that individual 14303 samples with reduced K/Th ratios are generated by AFC between 14321,1112 and average granite. Also, attention is called to the fact that 14303,277 falls in the Apollo 15 impact melt field.

The average REE patterns from 14303, 14304, and 14305, and those of 14168 and 14181 are presented in Fig. 9. We have attempted to model the REE profiles using the components and proportions of AFC determined in Figs. 5-8. There is reasonable agreement between measured and modeled REE profiles for 14168, 14181, 14303, and 14304. However, the average profile of the 14305 VHK basalts cannot be generated accurately by AFC between parental magma 14321,1161 and granite 73255c. The LREE of this profile are accurately modeled by using an average granite composition (as suggested in Fig. 6), whereas the HREE are best generated by using 73255c. It may be that the actual granite assimilant has a composition intermediate between these two, or the REE profile of the parental basalt (14321,1661) is not representative of the 14305 VHK parental magma.

IMPACT MELT ORIGIN FOR VHK BASALTS

The identification of 14303,277 as a probable impact melt highlights the importance of detailed geochemical analyses of the VHK basalts in order to determine the pristinity of these samples. It is important to note that only this sample has been defined as an impact melt, primarily because of the Ni/Co ratio and Au and Ir abundances. In Figs. 5-8, the bulk rock analysis of breccia 14303 (Brunfelt *et al.*, 1972) is plotted in order to determine whether the 14303 VHK basalts are crystalline products of remelted (via meteorite impact) matrix material. On Fig. 5, only two 14303 VHK basalts are plotted (.244 and .247), but neither of these has major elements composition similar to the bulk 14303 breccia. However, throughout Figs. 6-8, K/La, K/Hf, and K/Th ratios of 14303,277 and the bulk rock 14303 breccia support the contention that .277 is an impact melt. In fact, as shown in Fig. 8, this sample falls within the Apollo 15 impact melt field on a plot of K versus Th. No other reported VHK compositions can be regarded as impact melts, although Au and Ir abundances for the 14305 and 14168 VHK basalts are not reported.

DISCUSSION

The above modeling demonstrates that VHK basalt compositions can be generated by a combined assimilation and fractional crystallization process between a HA mare basalt parent magma and granite. The major element compositions of VHK basalts are generally very similar to the Apollo 14

HA mare basalts, consistent with the crystallization path described by Neal *et al.* (1987a). Only elevated K₂O contents give an indication as to the petrogenesis of these VHK basalts. Watson (1982) and Watson and Jurewicz (1984) have demonstrated that during granite assimilation by basaltic materials, the basalt becomes highly enriched in K with some depletion in Na. No real differences can be defined in Na abundance between VHK and HA mare basalts, but enrichment of K in the former appears to be indicative of granite assimilation.

In a study of HA mare basalt petrogenesis at the Apollo 14 site, Neal *et al.* (1987a) have proposed that the range of observed compositions is produced by an AFC process between a primitive magma and KREEP ($r = 0.22$). This requires that 14321,1443 and 14321,1112 compositions, taken as parental for the 14303 VHK basalts, already contain a KREEP component. Basalt 1443 has undergone 30% fractional crystallization (6.6% KREEP assimilation), whereas 1112 has undergone approximately 60% fractional crystallization (13.2% KREEP assimilation).

It is evident that VHK and HA mare basalts are genetically related at the Apollo 14 site. A primitive mare basalt magma evolves beneath the Apollo 14 site by combined AFC with KREEP to produce the array of HA mare basalt compositions. This primitive magma type may also undergo AFC with a granitic component, as VHK compositions 14168, 14181, 14303, and 14305 can be generated without any incorporated KREEP component. However, this primitive magma cannot produce the 14303 VHK compositions. These require a more evolved basalt parent (i.e., mare basalts with an assimilated KREEP component) and a different assimilated granite composition, corresponding to an average lunar granite. It is envisaged that in the dynamic process of AFC, KREEP is replaced by granite as the assimilated component during magma migration within the lunar crust. This produces the 14303 VHK basalts.

The rarity of both granite and VHK basalts in the lunar crust suggest that VHK basalt production is a highly localized phenomenon. Identification of both KREEP and granitic components in the 14303 VHK basalts indicates that *there must be at least two VHK basalt flows at the Apollo 14 site.*

The results of our research indicate that bulk granite assimilation can produce VHK basalts just as well as preferential incorporation of granitic feldspars. This observation is not at variance with the isotopic data reported by Shih *et al.* (1986, 1987). These authors conclude that at the time of crystallization, there is a dramatic increase in Rb/Sr ratio with little change in Sm/Nd ratio, attributing this to preferential assimilation of granitic feldspars. However, bulk granite has a relatively chondritic to slightly enriched Sm/Nd ratio (Fig. 4), similar to that of the parental basalts (especially 1443). Therefore, if bulk granite is combined with parental basalts used in this study, little alteration in Sm-Nd systematics will occur.

CONCLUSIONS

The above discussion outlines the importance of lunar granite in VHK basalt petrogenesis. However, unlike similar models, we have demonstrated that KREEP is also involved, and this

has major implications not only for VHK basalts, but also for KREEP-granite relationships (see #3 below). The main conclusions resulting from this study are as follows:

1. Major element compositions of VHK basalts fall along the general crystallization path proposed for Apollo 14 high Al (HA) mare basalts. Potassium is the only major element that deviates from a normal HA mare basalt composition. As the major elements in an AFC process can be effectively modeled by fractional crystallization alone, this suggests similar petrogeneses for VHK and HA basalts.

2. VHK basalts from breccias 14168, 14181, 14304, and 14305 are produced by combined assimilation and fractional crystallization of a primitive HA mare basalt magma (composition of 14321,1161) and granite (composition of 73255c).

3. VHK basalts from breccia 14303 are produced from a more evolved HA mare basalt magma (compositions of 14321,1443 and 14321,1161) and an average granite composition. This argues for these magmas to have resulted from normal Apollo 14 mare basalt evolution by AFC with KREEP. At a certain point along this evolutionary path, the KREEP assimilate is replaced by granite in the AFC process in order to produce VHK compositions. The actual AFC path taken is controlled not only by the composition of the parental magma, but also by the composition of the assimilated granite.

4. The different AFC components for 14168, 14181, 14304, and 14305 versus 14303 argue for at least two VHK basalt flows at the Apollo 14 site.

5. All reported VHK basalts are produced by granite assimilation. In this petrogenesis, the amounts of granite assimilation are small—i.e., maximum of 5.75% for 14303 VHK compositions. This process highlights the significance of the rare granite occurrences in the lunar crust.

6. The identification of 14303,277 as an impact melt highlights the importance of detailed geochemical analysis in determining the pristinity of VHK basalts.

Acknowledgments. This study would not have been possible without the capable assistance of the Planetary Materials Curatorial Staff at Johnson Space Center, especially Ms. Kim Willis. The sawing of the breccias, the elaborate documentation, and the actual "plucking" of the individual clasts was performed by Kim. We thank Randy Korotev at Washington University for assistance in the INA analyses, and Tom See at JSC for assistance in the fusion process for major element analyses. Acknowledgments are also due to John Shervais, Roman Schmitt, Gordon McKay, Graham Ryder, and John Jones for critical reviews and valuable discussions. The research reported in this paper was supported by NASA grants NGR 9-62 to L. A. Taylor and NAG 9-56 to L. A. Haskin.

REFERENCES

- Arth J. G. and Hanson G. N. (1975) Geochemistry and origin of the early Pre-Cambrian crust of north-eastern Minnesota. *Geochim. Cosmochim. Acta* 39, 325-362.
- Bence A. E. and Papike J. J. (1972) Pyroxenes as recorders of lunar basalt petrogenesis: Chemical trends due to crystal-liquid interactions. *Proc. Lunar Sci. Conf. 3rd*, 431-469.

- Binder A. B. (1982) The mare basalt magma source region and mare basalt magma genesis. *Proc. Lunar Planet. Sci. Conf. 13th*, in *J. Geophys. Res.*, 87, A37-A53.
- Binder A. B. (1985) Mare basalt genesis: Modeling trace elements and isotopic ratios. *Proc. Lunar Planet. Sci. Conf. 16th*, in *J. Geophys. Res.*, 90, D19-D30.
- Blanchard D. P. and Budahn J. R. (1979) Remnants from the ancient lunar crust: clasts from consortium breccia 73255. *Proc. Lunar Planet. Sci. Conf. 10th*, 803-816.
- Brunfelt A. O., Heier K. S., Nilssen B., and Sundvoll B. (1972) Distribution of elements between different phases of Apollo 14 rocks and soils. *Proc. Lunar Sci. Conf. 3rd*, 1133-1147.
- DePaolo D. J. (1981) Trace element and isotopic effects of combined wallrock assimilation and fractional crystallization. *Earth Planet. Sci. Lett.*, 53, 189-202.
- Dickinson T., Taylor G. J., Keil K., Schmitt R. A., Hughes S. S., and Smith M. R. (1985) Apollo 14 aluminous mare basalts and their possible relationship to KREEP. *Proc. Lunar Planet. Sci. Conf. 16th*, in *J. Geophys. Res.*, 90, C365-C374.
- Drake M. J. and Weill D. F. (1975) Partition of Sr, Ba, Ca, Y, Eu²⁺ and Eu³⁺, and other REE between plagioclase feldspar and magmatic liquid: an experimental study. *Geochim. Cosmochim. Acta*, 39, 689-712.
- El Goresy A., Taylor L. A., and Ramdohr P. (1972) Fra Mauro crystalline rocks: Mineralogy, geochemistry, and subsolidus reduction of opaque minerals. *Proc. Lunar Sci. Conf. 3rd*, 333-348.
- Goldstein J. I. and Yakowitz H. (1971) Metallic inclusions and metal particles in the Apollo 12 lunar soil. *Proc. Lunar Sci. Conf. 2nd*, 177-191.
- Goodrich C. A., Taylor G. J., Keil K., Kallemeyn G. W., and Warren P. H. (1986) Alkali norite, troctolites, and VHK mare basalts from breccia 14304. *Proc. Lunar Planet. Sci. Conf. 16th*, in *J. Geophys. Res.*, 91, D305-D318.
- Haskin L. A. and Korotev R. L. (1977) Test of a model for trace element partition during closed-system solidification of a silicate liquid. *Geochim. Cosmochim. Acta*, 41, 921-939.
- Irving A. J. and Frey F. A. (1984) Trace element abundances in megacrysts and their host basalts: Constraints on partition coefficients and megacryst genesis. *Geochim. Cosmochim. Acta*, 48, 1201-1221.
- Kesson S. E. (1975) Mare basalts: melting experiments and petrogenetic interpretations. *Proc. Lunar Sci. Conf. 6th*, 921-944.
- Lindstrom M. M. (1984) Alkali gabbronorite, ultra-KREEPy melt rock, and the diverse suite of clasts in North Ray Crater feldspathic fragmental breccia 67975. *Proc. Lunar Planet. Sci. Conf. 15th*, in *J. Geophys. Res.*, 89, C50-C62.
- Lindstrom M. M. and Haskin L. A. (1978) Causes of compositional variations within mare basalt suites. *Proc. Lunar Planet. Sci. Conf. 9th*, 465-486.
- Lindstrom D. J. and Korotev R. L. (1982) TEABAGS: Computer programs for instrumental neutron activation analysis. *J. Radioanal. Chem.* 70, 439-458.
- Longhi J. (1977) Magma oceanography 2: Chemical evolution and crustal formation. *Proc. Lunar Sci. Conf. 8th*, 601-621.
- McKay G. A., Wagstaff J., and Yang S.-R. (1986) Zr, Hf, and REE partition coefficients for ilmenite and other minerals in high-Ti lunar mare basalts: an experimental study. *Proc. Lunar Planet. Sci. Conf. 16th*, in *J. Geophys. Res.*, 91, D229-D237.
- Neal C. R., Taylor L. A., and Lindstrom M. M. (1987a) Mare basalt petrogenesis: Assimilation of KREEP-like components by a fractionating magma. *Proc. Lunar Planet. Sci. Conf. 18th*, this volume.
- Neal C. R., Taylor L. A., and Lindstrom M. M. (1987b) Very High Potassium (VHK) basalt petrogenesis: The role of granite and KREEP components (abstract). In *Lunar and Planetary Science XVIII*, pp. 710-711. Lunar and Planetary Institute, Houston.
- Nyquist L. E., Shih C.-Y., Wooden J. L., Bansal B. M., and Weismann H. (1979) The Sr and Nd isotopic record of Apollo 12 basalts: Implications for lunar geochemical evolution. *Proc. Lunar Planet. Sci. Conf. 10th*, 77-114.
- Ringwood A. E. and Kesson S. E. (1976) A dynamic model for mare basalt petrogenesis. *Proc. Lunar Sci. Conf. 7th*, 1697-1722.
- Ryder G. and Spudis P. (1987) Chemical composition and origin of Apollo 15 impact melts. *Proc. Lunar Planet. Sci. Conf. 17th*, in *J. Geophys. Res.*, 92, E432-E446.
- Ryder G., Norman M. D., and Score R. A. (1980) The distinction of pristine from meteorite-contaminated highland rocks using metal compositions. *Proc. Lunar Planet. Sci. Conf. 11th*, 471-480.
- Salpas P. A., Shervais J. W., Knapp S. A., and Taylor L. A. (1985) Petrogenesis of lunar granites: The results of apatite fractionation (abstract). In *Lunar and Planetary Science XVI*, pp 726-727. Lunar and Planetary Institute, Houston.
- Schnetzler C. C. and Philpotts J. A. (1970) Partition coefficients of REE between igneous matrix material and rock-forming mineral phenocrysts - II. *Geochim. Cosmochim. Acta*, 34, 331-340.
- Shervais J. W., Taylor L. A., Laul J. C., and Smith M. R. (1984) Pristine highland clasts in consortium breccia 14305: Petrology and geochemistry. *Proc. Lunar Planet. Sci. Conf. 15th*, in *J. Geophys. Res.*, 89, C25-C40.
- Shervais J. W., Taylor L. A., and Lindstrom M. M. (1985a) Apollo 14 mare basalts: Petrology and geochemistry of clasts from consortium breccia 14321. *Proc. Lunar Planet. Sci. Conf. 15th*, in *J. Geophys. Res.*, 90, C375-C395.
- Shervais J. W., Taylor L. A., Laul J. C., Shih C.-Y., and Nyquist L. E. (1985b) Very High Potassium (VHK) basalt: Complications in mare basalt petrogenesis. *Proc. Lunar Planet. Sci. Conf. 16th*, in *J. Geophys. Res.*, 90, D3-D18.
- Shih C.-Y., Nyquist L. E., Bogard D. D., Bansal B. M., Weismann H., Johnson P., Shervais J. W., and Taylor L. A. (1986) Geochronology and petrogenesis of Apollo 14 Very High Potassium mare basalts. *Proc. Lunar Planet. Sci. Conf. 16th*, in *J. Geophys. Res.*, 91, D214-D228.
- Shih C.-Y., Nyquist L. E., Bogard D. D., Dasch E. J., Bansal B. M., and Weismann H. (1987) Geochronology of high-K aluminous mare basalt clasts from Apollo 14 breccia 14303. *Geochim. Cosmochim. Acta*, in press.
- Vaniman D. T. and Papike J. J. (1980) Lunar highland melt rocks: Chemistry, petrology, and silicate mineralogy. *Proc. Conf. Lunar Highlands Crust (J. J. Papike and R. B. Merrill, eds.)*, pp. 271-337. Pergamon, New York.
- Villemant B., Jaffrezic H., Joron J. L., and Treuil M. (1981) Distribution coefficients of major and trace elements: fractional crystallization in the alkali basalt series of Chaîne des Puys (Massif Central, France). *Geochim. Cosmochim. Acta*, 45, 1997-2016.
- Walker D., Longhi J., and Hays J. R. (1972) Experimental petrology and origin of Fra Mauro rocks and soil. *Proc. Lunar Sci. Conf. 3rd*, 797-817.
- Walker D., Longhi J., Grove T. L., Stolper E., and Hays J. F. (1973) Experimental petrology and origin of rocks from the Descartes Highlands. *Proc. Lunar Sci. Conf. 4th*, 1013-1032.
- Warner R. D., Taylor G. J., Keil K., Ma M.-S., and Schmitt R. A. (1980) Aluminous mare basalts: New data from Apollo 14 coarse fines. *Proc. Lunar Planet. Sci. Conf. 11th*, 87-104.
- Warren P. H. and Wasson J. T. (1979) Effects of pressure on the crystallization of a "chondritic" magma ocean and implications for the bulk composition of the Moon. *Proc. Lunar Planet. Sci. Conf. 10th*, 2051-2083.
- Warren P. H., Taylor G. J., Keil K., Kallemeyn G. W., Shirley D. N., and Wasson J. T. (1983a) Seventh foray: Whitlockite-rich lithologies,

- a diopside-bearing troctolitic anorthosite, ferroan anorthosites, and KREEP. *Proc. Lunar Planet. Sci. Conf. 14th*, in *J. Geophys. Res.*, **88**, B151-B164.
- Warren P. H., Taylor G. J., and Keil K. (1983b) Regolith breccia Allan Hills A81005: Evidence of lunar origin, and petrography of pristine and non-pristine clasts. *Geophys. Res. Lett.*, **10**, 779-782.
- Warren P. H., Taylor G. J., Keil K., Shirley D. N., and Wasson J. T. (1983c) Petrology and chemistry of two "large" granite clasts from the Moon. *Earth Planet. Sci. Lett.*, **64**, 175-185.
- Warren P. H., Taylor G. J., Keil K., Kallemeyn G. W., Shirley D. N., and Wasson J. T. (1983d) Seventh foray: Whitlockite-rich lithologies, a diopside-bearing troctolitic anorthosite, ferroan anorthosites and KREEP. *Proc. Lunar Planet. Sci. Conf. 14th*, in *J. Geophys. Res.*, **88**, B151-B164.
- Warren P. H., Shirley D. N., and Kallemeyn G. W. (1986) A potpourri of pristine moon rocks, including a VHK mare basalt and a unique, augite-rich Apollo 17 anorthosite. *Proc. Lunar Planet. Sci. Conf. 16th*, in *J. Geophys. Res.*, **91**, D319-D330.
- Watson E. B. (1982) Basalt contamination by continental crust: some experiments and models. *Contrib. Mineral. Petrol.*, **80**, 73-87.
- Watson E. B. and Jurewicz S. R. (1984) Behaviour of alkalis during diffusive interaction of granitic xenoliths with basaltic magma. *J. Geol.*, **92**, 121-131.